Perception, 2001, volume 30, pages 833 – 853

DOI:10.1068/p3164

Processing time of contour integration: the role of colour, contrast, and curvature†

William H A Beaudot, Kathy T Mullen
McGill Vision Research, Department of Ophthalmology, McGill University, 687 Pine Avenue West, H4-14, Montréal, Québec H3A 1A1, Canada; e-mail: wbeaudot@vision.mcgill.ca
Received 27 November 2000, in revised form 14 February 2001

Abstract. We investigated the temporal properties of the red – green, blue – yellow, and luminance mechanisms in a contour-integration task which required the linking of orientation across space to detect a 'path'. Reaction times were obtained for simple detection of the stimulus regardless of the presence of a path, and for path detection measured by a yes/no procedure with path and no-path stimuli randomly presented. Additional processing times for contour integration were calculated as the difference between reaction times for simple stimulus detection and path detection, and were measured as a function of stimulus contrast for straight and curved paths. We found that processing time shows effects not apparent in choice reaction-time measurements. (i) Processing time for curved paths is longer than for straight paths. (ii) For straight paths, the achromatic mechanism is faster than the two chromatic ones, with no difference between the red – green and blue – yellow mechanisms. For curved paths there is no difference in processing time between mechanisms. (iii) The extra processing time required to detect curved compared to straight paths is longest for the achromatic mechanism, and similar for the red – green and blue – yellow mechanisms. (iv) Detection of the absence of a path requires at least 50 ms of additional time independently of chromaticity, contrast, and path curvature. The significance of these differences and similarities between postreceptoral mechanisms is discussed.

1 Introduction

A contour-integration paradigm, relying on the spatial integration of co-oriented and collinear cues across the visual field, has been extensively used to investigate the spatial properties of the linking process involved in contour-based shape perception (Dakin and Hess 1998, 1999; Field et al 1993; Kapadia et al 1995; Kovacs and Julesz 1993; McIlhagga and Mullen 1996; Mullen et al 2000; Pettet 1999; Pettet et al 1998; Williams and Hess 1998). In only a few studies, however, have the temporal properties of this process been investigated, and these have concentrated on the effects of different exposure durations (Braun 1999; Hess et al 2001), temporal frequency (Hess et al 2001), or onset asynchrony (Beaudot, in revision) on performance. Yet many of the recent models of contour integration have implicit dynamic components requiring time to execute the process, for example, by using any iterative computation (Parent and Zucker 1989; Shashua and Ullman 1988), 'fast plasticity' (Braun et al 1994), the cumulative effects of local interactions propagating along the contour (Pettet et al 1998; Roelfsema and Singer 1998), or temporal synchronisation (Li 1998; Yen and Finkel 1998). None has yet incorporated explicit dynamics such the curvature-dependent dynamics reported by Hess et al (2001) for achromatic contour integration. A study of the temporal dynamics of contour integration in colour vision will thus potentially provide more insight into the implicit or explicit nature of the dynamic processes.

In previous work we have investigated the roles of the three postreceptoral mechanisms (red – green, blue – yellow, and luminance) in contour integration using the stimulus shown in figure 1 (McIlhagga and Mullen 1996; Mullen et al 2000). We demonstrated that, despite differences in anatomical and physiological precortical factors,

† This work was initially reported to the 1999 Meeting of the Association for Research in Vision and Ophthalmology, Fort Lauderdale, Florida, USA (IOVS 40/4, S809).

the three postreceptoral mechanisms can all support contour integration at very similar levels of performance. All three mechanisms are affected similarly by curvature and contrast, and all are similarly affected by the addition of orientation noise, implying that they have similar sampling efficiencies and internal noises for contour integration (Mullen et al 2000). Despite these similarities, however, linking between postreceptoral mechanisms is very disruptive to contour integration: if the path elements alternate between two postreceptoral mechanisms (eg red – green and blue – yellow) performance decreases dramatically (McIlhagga and Mullen 1996; Mullen et al 2000). Having established the spatial properties between the postreceptoral mechanisms, we now investigate their dynamics.

In this paper, we use reaction times as a basis for calculating the 'processing time' of the red – green, blue – yellow, and luminance mechanisms for contour integration. Measurements of reaction times per se are not a good measure for investigating the processing speed of the different mechanisms since reaction times consist of multiple components (perceptual integration time, transmission time, delay in response process, the motor response) which may differ across mechanisms. Moreover, reaction time is not always correlated with the perceptual latency of a stimulus (Ejima and Ohtani 1987). To overcome this problem, we first obtained reaction times for simple detection of the stimulus array without asking the subject to determine the presence of a path. We then obtained reaction times for path detection, in which the subject was asked to determine the presence of a path. We estimated the additional processing time for contour integration compared with simple stimulus detection, by subtracting reaction times for simple stimulus detection from the path-detection reaction times. Under the assumption of serial processing (ie path detection following simple detection) this additional processing time for contour integration would be the processing time *specific* to contour integration. Although a strict serial processing is the simplest assumption, contour integration may in fact be underway before stimulus detection is completed. It is thus likely that stimulus detection and contour integration share or perform some common functions, other than precortical and motor processes, such as contrast integration for example. The additional processing time should still account for the time demand of contour integration. Our main assumption relies then on a weak form of the *subtractive method* proposed by Donders (1868) (see Protocol, section 2.4).

In this paper we have two parallel aims. The first is to determine the additional processing times for contour integration for the three postreceptoral mechanisms, and to this end we perform all our experiments with three cardinal stimuli (red – green, blue – yellow, and achromatic). Our second aim is to determine how curvature of the contour affects the additional processing time, and for this we use two path curvatures, one producing a relatively straight contour, and the other producing a more curved one. Since contrast is also an important variable affecting reaction time, we make our measurements over a wide range of different cone contrasts for each mechanism, and take the effects of contrast into account to obtain contrast-independent measures of processing time.

2 Methods

2.1 *Stimuli*

The stimuli were square patches (14 deg $\times$ 14 deg) of pseudorandomly distributed Gabor elements (figure 1a). The subject's task was to detect a 'path' which consisted of a set of ten oriented Gabor elements aligned along a common contour, embedded in the background of similar but randomly oriented Gabor elements. Inspection of figure 1a reveals that the path in the example winds horizontally across the figure. Gabor elements were used to limit the spatial bandwidth of the stimuli (Field et al 1993; McIlhagga

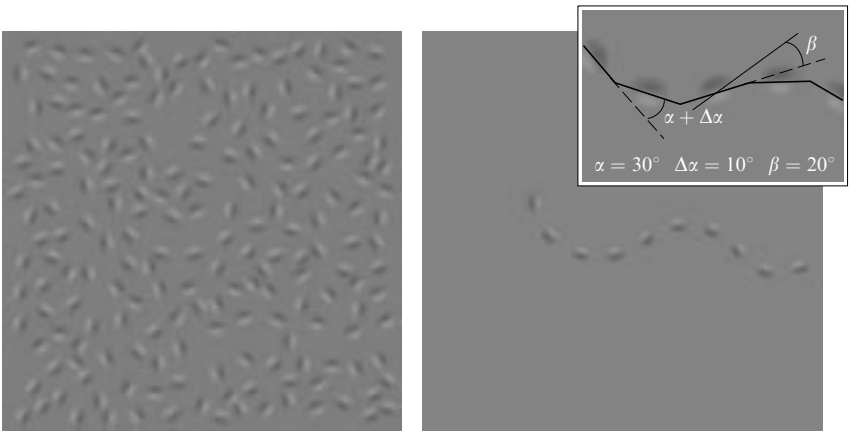

(a) Stimulus example (b) Path construction

Figure 1. (a) An example of a stimulus. The 'path' is difficult to detect when embedded in a background of similar but randomly oriented elements. Experienced subjects perform at around 65%–75% correct under a steady presentation of 500 ms. (b) The path is shown separated from the background elements. It is a chain of ten Gabor elements which vary systematically in their orientation, as described in the inset. Inset: the path is made up of ten backbone line segments. The orientation difference between each successive line segment is given by the angle α which in this case is $\pm 30^\circ$. α determines the path curvature. $\Delta\alpha$ is a small orientation jitter added to α and is uniformly distributed between $\pm 10^\circ$. β gives the orientation of the Gabor element with respect to the backbone element. β is zero in experiments presented in this paper. Note that Gabor elements of all paths are odd-symmetric and aligned in phase.

and Mullen 1996; Mullen et al 2000). The elements were odd symmetric and defined by the equation:

$$g(x, y, \theta) = c \sin[2\pi f(x \sin\theta + y \cos\theta)] \exp\left(-\frac{x^2 + y^2}{2\sigma^2}\right), \quad (1)$$

where θ is the element orientation, (x, y) is the distance in degrees from the element centre, and c is the contrast. The sinusoidal frequency (f) is 1.5 cycles deg^{-1}, and the space constant (σ) is 0.17 deg.

A yes/no procedure was used to measure the subject's ability to detect the path by discriminating between the path stimulus and a no-path stimulus which consisted only of randomly placed Gabor elements. The no-path stimulus was constructed with the following algorithm. The stimulus area was divided into a 14×14 grid of equally sized cells (each 1 deg $\times$ 1 deg). A Gabor element of random orientation was placed in each cell with the restriction that each cell contained the centre of only one Gabor element. This pseudorandom placement prevents clumping of the elements. Overlap of the elements was also prevented by restricting the placement of their centres within the cell. It was sometimes impossible to place a Gabor element in its cell because it would be too close to elements previously placed. This produced an empty cell, and no more than eight empty cells were permitted in a display and the average number was four. The average distance between neighbouring Gabor elements was 1.3 deg.

The path stimulus can be considered as two parts, the ten path elements themselves and the background elements. A set of path elements is shown in figure 1b, and its construction is illustrated in the inset. The path has a 'backbone' of ten invisible line segments, and each line segment is randomly selected to be between 1.2 and 1.4 deg long. The shape of the backbone is controlled by the parameter α (curvature) which determines the angle difference between adjacent backbone elements. Higher values of α produce more curvature in the path, and lower values produce straighter paths.

In this paper only two curvatures are used: 0°, defining 'straight' paths, and 20° defining 'curved' paths (see figure 1). We showed in a previous study that 20° is a curvature threshold for contour integration, independent of postreceptoral mechanisms and contrasts, corresponding to a significant drop of 18.4% in performance compared with the straight condition (Mullen et al 2000). To avoid the occurrence of absolutely straight paths when α is 0°, an orientation jitter uniformly distributed between $\pm 10°$ was added to α. Gabor elements were placed in the middle of each line segment with the same orientation. Finally, to avoid random closure of the paths with a high curvature, which can affect detection (Elder and Zucker 1993; Kovacs and Julesz 1993), paths which looped back on themselves were discarded and new ones generated. The entire path was pasted into the display at a random location, making sure that the centres of the Gabor elements occupied different cells, and that at least one path element passed through the central region of the stimulus (defined as a circular region 3 deg in diameter). The remaining empty cells were filled with randomly oriented Gabor elements, as in the no-path stimulus.

Various control measurements ensured that no spurious cues could be used for path detection. In particular, we ascertained that the presence of the path does not affect the local densities of the elements since the averaged distance between path elements and between background elements is the same and the number of empty neighbouring cells are the same for both path and background elements. Furthermore, the number of empty cells is the same for both path and no-path stimuli, indicating no global density changes. If neither density nor proximity are cues, path visibility should be due only to the alignment of the elements of the path since nothing else distinguishes path element from background element. This was confirmed in a control experiment in which the orientation of the path elements was randomised. The path could not be detected under extended viewing regardless of the curvature. The continuity in the local orientation across space is, then, a crucial feature for path detection.

2.2 *Chromatic representation of the stimuli*

The chromaticity of the stimuli was defined in three-dimensional cone contrast space in which each axis represents the quantal catch of the long (L), medium (M), and short (S) wavelength cone types normalised with respect to the white background. Stimulus chromaticity and contrast is given by a vector direction and magnitude, respectively, within the cone contrast space. In all experiments only the three cardinal stimuli were used. These are designed to isolate each of the three different postreceptoral mechanisms. A cardinal direction for a given mechanism is the unique direction orthogonal to the vector directions of the other two mechanisms. Previous studies have estimated the red–green, blue–yellow, and luminance mechanism directions to be approximately: $L - M$; $S - 0.5(L + M)$; and $3L + M$ (Cole et al 1993; Sankeralli and Mullen 1996). From these, the calculated luminance and blue–yellow cardinal directions are $L + M + S$ (the achromatic direction) and S, respectively. The wide intersubject variability found for the luminance mechanism affects the specification of the red–green cardinal direction. The red–green isoluminant direction was determined for each subject individually with a motion-nulling technique (Anstis and Cavanagh 1983) for a patch of grating (1.5 cycles deg^{-1}, 3.6 deg^2) viewed binocularly and foveally, and having the same mean luminance and chromaticity as the Gabor stimuli used in the experiments. Since the red–green isoluminant direction was specified within the L–M cone contrast plane, it was not orthogonal to the blue–yellow mechanism. Any resulting cross stimulation of the blue–yellow mechanism would be small, however, and, given the very low cone contrast sensitivity of the blue–yellow mechanism relative to the red–green mechanism (Sankeralli and Mullen 1996), is highly unlikely to influence the results. Maximum contrast

for red – green stimuli was limited by the display and varied across subjects according to their red – green isoluminant axis.

2.3 *Apparatus and calibrations*

Stimuli were displayed on a Sony Trinitron monitor driven by a VSG 2/4 graphics board (Cambridge Research Systems) with 15 bits contrast resolution, housed in a Pentium PC computer. The frame rate of the display was 76 Hz. The spectral emissions of the red, green, and blue guns of the monitor were calibrated at the National Research Council of Canada with a Photo Research PR-700-PC SpectraScan. The monitor was gamma corrected in software with lookup tables which used luminance measurements obtained from a United Detector Technology Optometer (UDT S370) fitted with a 265 photometric sensor. The Smith and Pokorny fundamentals (Smith and Pokorny 1975) were used for the spectral absorption of the L, M, and S cones. From these data a linear transform was calculated to specify the phosphor contrasts required for given cone contrasts (Cole and Hine 1992). The monitor was viewed in a blacked-out room. The mean luminance of the display was 14.2 cd m^{-2}. The stimuli were viewed at 60 cm, and subtended a constant area of 504 pixels $\times$ 504 pixels (14 deg $\times$ 14 deg). Stimuli were generated on-line, and a new stimulus was generated for each presentation. Reaction times were measured by pressure on one of the two mouse buttons under Windows 95 through 32 bits-mode functions.

2.4 *Protocol*

Reaction times were obtained as a function of stimulus contrast and curvature for (1) simple detection of the stimulus array regardless of the presence of a path, and (2) detection of the presence of a path in the stimulus array. By differencing these two measures $(2 - 1)$, we derived the additional processing time for contour integration. Thus processing time is the time required specifically for integration of the Gabor elements into a contour. Processing time also includes any difference in decision time of higher processes between simple and path detections, but excludes the times required for simple stimulus detection (the sensory process) and manual response execution (the motor process). The motor process is thought to be invariant with the visual properties of the stimuli and the type of task (simple detection or discrimination). The subtractive method follows, for example, that of Greenlee and Breitmeyer (1989), and is originally based on the fact reported by Donders (1868) that a simple reaction time is shorter than a choice reaction time, and that the recognition reaction time is the longest of all. There are, however, some potential difficulties [such as anticipation errors or the additivity of the times of mental events (see Külpe 1893)] with Donders' subtractive method that may apply to the differencing of path detection and simple reaction times. They are addressed below.

For reaction times for simple stimulus detection, the subjects had to respond by pressing a mouse button as soon as they saw the stimulus array. They were asked to divide their responses equally between their left and right hands by pressing the left or right mouse buttons in alternation. This allowed us to assess any differences in reaction time between left and right hand responses that might contaminate the yes/no procedure used for path detection. Reaction times were then obtained for path detection, measured by a yes/no procedure with path and no-path stimuli randomly presented. Subjects were asked to press the left or the right button (with the left or right hand, respectively) to indicate whether or not the stimulus contained a path. These two experiments were always performed sequentially for each contrast and curvature condition to control for the effects of the normal variability of reaction times.

In both experiments, half the presented stimuli contained the 'path', made of ten adjacent aligned elements, and the other half had no path, presented randomly in each session. Stimuli were presented abruptly, and were response terminated. Subjects had

to press one of the mouse buttons to pass to the next trial that began after a random duration (250 – 750 ms), from which one can estimate the tendency for a subject to make an anticipation error. The number of trials per session for each experiment was fifty for each subject, and three to four sessions were performed for each condition on average. Subjects were asked to respond as fast and reliably as possible. Auditory feedback was given after each trial. A black fixation mark was presented briefly at the beginning of each session in the centre of the display, and subjects were asked to sustain their focus during the whole session. In the different experiments, the two path curvatures (0° and 20°) and a range of contrasts were used. Practice trials were run before the experiments commenced.

We verified that subjects did not change their criteria for path detection across conditions, and that subjects showed similar criteria. We computed the response bias[(1)] for path detection for each subject under all conditions in our data. We find no significant differences in criterion for any condition or subject. All the reaction-time data for path detection are therefore comparable. Reaction times were then analysed in the following way. We first canceled sessions for path discrimination for which performance was less than 60%. This affected conditions with lowest contrast and highest curvature. Reaction times for false-positive and negative responses for path detection were eliminated, so only reaction times for valid responses remained. Reaction times for each experimental condition (contrast and curvature) were combined across valid sessions. The mean and standard deviation were computed. Reaction times below 100 ms (anticipatory responses) and larger than two standard deviations above the mean (late responses) were removed. The median value of the subsequent distribution was then computed, and used as an estimation of the reaction time for each condition. We addressed the difficulties of the subtractive method in the following way. (i) We removed the reaction times from anticipatory and late responses from the data to avoid any contamination. Note, however, that our subjects showed very small rates of anticipatory responses (less than 3% for simple detection and none at all for path detection irrespective of the mechanism or contrast) and late responses (less than 2% irrespective of the condition or subject). (ii) The fact that no anticipatory responses at all were given for the path-detection task indicates clearly that the subjects have perfectly integrated the element contrast before giving their response for path detection, that is their detection was prerequisite. This is also supported by the fact that path detection is relatively independent of element contrast (Hess et al 2001; Mullen et al 2000). The assumption that contour integration requires stimulus detection is then quite reasonable.

As reaction time declined with increasing stimulus contrast to reach asymptotic levels (see figures 2 and 4), in accordance with previous studies (Burr et al 1998; Ejima and Ohtani 1987), the variation in reaction time with stimulus contrast can be well characterised by a simple descriptive model with three parameters (Barbur et al 1998):

$$\mathrm{RT}(x) = c_1 \exp(-x c_2) + c_3 \,, \tag{2}$$

where x represents the contrast of the elements, c_1 and c_2 determine the initial amplitude and rate of decay, respectively, and c_3 determines the asymptotic reaction time. We fitted this function to the reaction-time data for simple stimulus detection and path detection. In the subsequent analysis we consider the asymptotic reaction time as the most relevant measure of the perceptual latency since, for low contrasts, simple reaction time could have been affected differently by the different criteria involved in the task, for example detection criterion and reaction criterion (Ejima and Ohtani 1987).

[(1)] The response bias c was defined by $c = -0.5[z(\mathrm{H}) + z(\mathrm{F})]$, where $z(\mathrm{H})$ and $z(\mathrm{F})$ are the z-score for the hit rate (correct YES responses) and the false-alarm rate (calculated as 1 – correct NO responses) respectively.

We employed the same equation (2) to fit the data for the additional processing times since the majority of them (especially the chromatic data) show the same contrast dependence as the reaction times, namely a monotonic decrease with contrast.[(2)]

However, in some cases, especially for the red–green and blue–yellow stimuli, asymptotic performance could not be reached satisfactorily with increasing contrast. Maximum cone contrast for chromatic stimuli is limited by the display, and this sometimes prevents the minimum reaction time for the red–green and blue–yellow mechanisms being reached. In these cases, the best fits by equation (2) provide an extrapolation of the asymptotic level. To overcome this limitation, we also compare discrimination reaction times and processing times at a multiple of path-detection threshold. Contrast thresholds for path detection were measured in a temporal two-alternative forced-choice (2AFC) experiment with a 500 ms presentation for both 0° and 20° path curvatures and for each subject, as described previously (Mullen et al 2000).

2.5 *Observers*

The observers were two naïve volunteers (JAC and JLF) and the two authors (WB and KTM). All four have normal, or refracted-to-normal vision, and all have normal colour vision according to the Farnsworth–Munsell 100-Hue Test. All experiments were done under binocular conditions. Naïve subjects were trained in a temporal 2AFC experiment to reach performance levels at least identical to those of the two authors.

3 Results

3.1 *Reaction time for simple stimulus detection*

Reaction times for simple stimulus detection are shown in figure 2 by data points, with solid and dashed curves denoting fits of equation (2). Reaction times for simple stimulus detection are very similar across the four subjects. Simple reaction times are expressed as function of absolute cone contrast for two curvatures for each cardinal stimulus (red–green, blue–yellow, and achromatic). All mechanisms at all curvatures show a decrease in reaction time with increasing contrast, varying between 250 and 400 ms for the range of contrasts used in the experiment. There is no difference between right and left hands or between straight and curved path conditions, as expected since stimulus content in terms of spatial configuration should not be relevant to simple stimulus detection. Reaction times for achromatic stimuli asymptote at 250–300 ms, while for chromatic stimuli (red–green and blue–yellow) reaction times converge at or above 300 ms.

Reaction times for the three mechanisms are displaced differentially along the cone contrast axis, in part because of their different cone contrast thresholds. As a consequence, if compared at the same absolute cone contrast, reaction times for blue–yellow stimuli will appear as longer than reaction times for the achromatic and red–green stimuli. The differences in contrast sensitivity between the postreceptoral mechanisms, and all contrast effects on reaction time, can be taken into account by considering asymptotic reaction times, which are not contrast dependent. Asymptotic simple reaction times were derived by fitting the function given by equation (2), and the values were averaged across subjects, as shown in figure 3. We applied separate

[(2)] It would have been reasonable to fit our processing times, which were calculated as the difference between reaction times, as a difference of exponentials (DoE) [ie difference of equation (2) with respective values of c_i]. However, this does not apply very well to processing times for chromatic data (see figure 6) because they show the same monotonic decrease with contrast as the reaction times whereas a DoE fit predicts a variety of shapes, among which is a U-shaped function. The fitting by a DoE would be then underconstrained, ie have too many parameters. Only processing times for achromatic data show a slightly U-shaped dependence on contrast, which could be explained, if significant, by a DoE. In the results section (table 1), however, we also provide statistics on the minimum processing times derived from the fitting of a DoE to achromatic data.

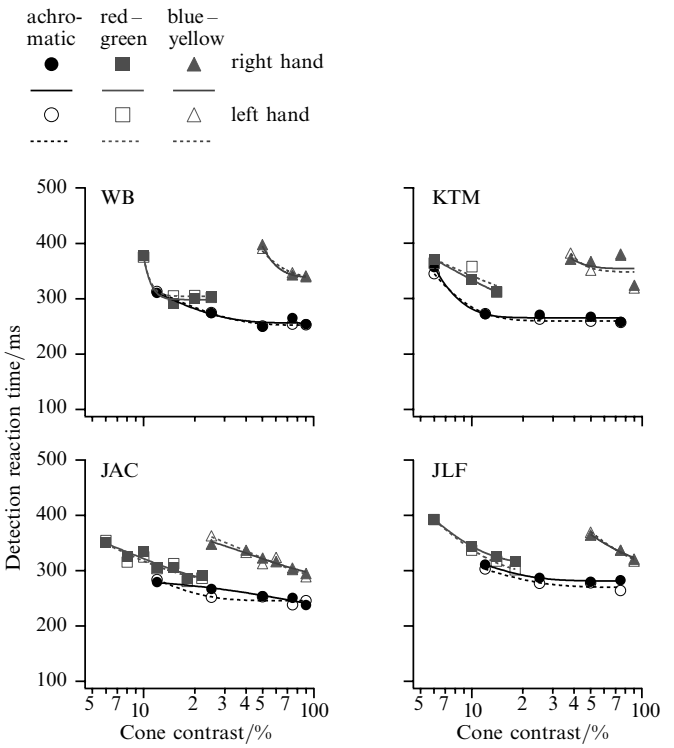

(a) Straight-path detection

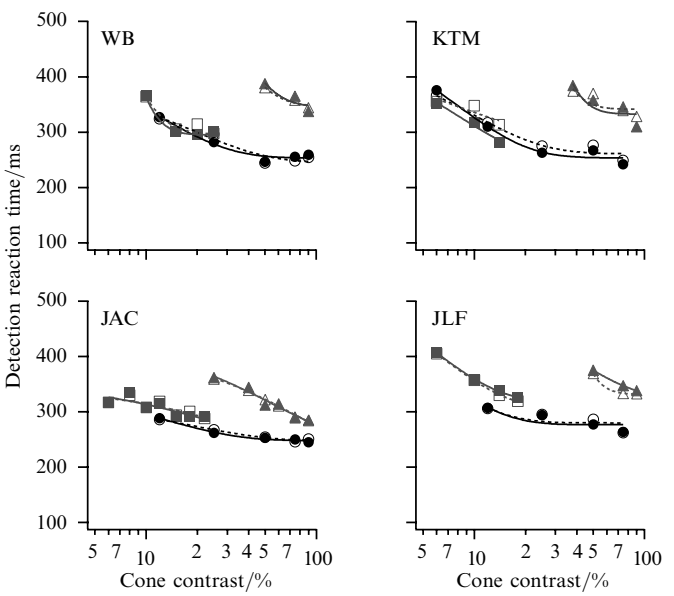

(b) Curved-path detection

Figure 2. Simple reaction times as a function of contrast for all four subjects. Reaction times for simple stimulus detection for straight (a) and curved (b) path conditions expressed as a function of absolute cone contrast. Circles, squares, and triangles represent simple reaction times for achromatic, red – green, and blue – yellow stimuli, respectively. Plain and open symbols represent measurements of right-hand and left-hand reaction times, respectively. Solid and dashed lines denote fits of equation (2) (see section 2) of the right-hand and left-hand reaction times, respectively.

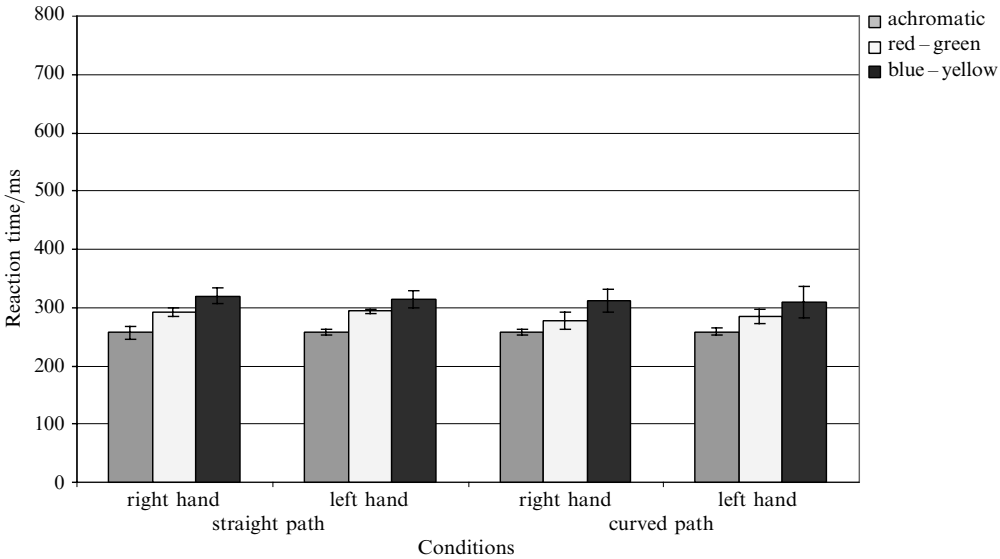

Figure 3. Averaged asymptotic simple reaction times across subjects. Asymptotic reaction times were derived by fitting equation (2) to the data in figure 2. Each experimental condition is represented from left to right: right-hand and left-hand detections of straight paths, right-hand and left-hand detections of curved paths. Error bars denote standard errors of the means.

one-way repeated-measures ANOVAs for each chromatic mechanism to show that there are no significant differences in asymptotic reaction times between the averaged left and right hand responses, or between the averaged straight (0°) and curved (20°) path responses. We also collapsed data across these two conditions (hand and path curvature) and applied a further one-way repeated-measures ANOVA to test differences in asymptotic reaction times between the three chromatic mechanisms. A significant main effect of chromatic mechanism was found ($F_{2,30} = 27.226$, $p < 0.0001$). Differences between mechanisms were further explored with a Tukey – Kramer a posteriori analysis with a 5% significance level which showed that the asymptotic reaction time for achromatic stimuli is significantly shorter than for both red – green (by 29 ms) and blue – yellow stimuli (by 56 ms), and that the asymptotic reaction time for red – green stimuli is significantly shorter than for the blue – yellow stimuli (by 27 ms). The averaged reaction times are: 257 ± 6 ms (achromatic), 287 ± 12 ms (red – green), and 314 ± 13 ms (blue – yellow).

3.2 *Reaction time for path/no-path discrimination*

Reaction times for path/no-path discrimination are plotted in figure 4 as a function of multiples of cone contrast thresholds by data points, with solid and dashed curves denoting fits of equation (2). Similarly to simple reaction times, path-discrimination reaction times show a decrease with increasing contrast for the three postreceptoral mechanisms. For the range of contrasts we used, all reaction times for path discrimination are above 375 ms, and consequently are significantly longer than the reaction times for simple stimulus detection. They also show a steeper increase at low contrasts for all conditions, suggesting that discrimination reaction times are more sensitive to contrast. There is, however, a greater variability across subjects for the discrimination task than for the simple stimulus detection. Under equivalent conditions (same multiples of path-detection threshold), reaction times for achromatic stimuli are always shorter than for chromatic stimuli for all subjects, the difference varying across subjects and curvature conditions. However, only discrimination reaction times for the luminance mechanism reach clearly an asymptotic level at higher contrasts for all conditions.

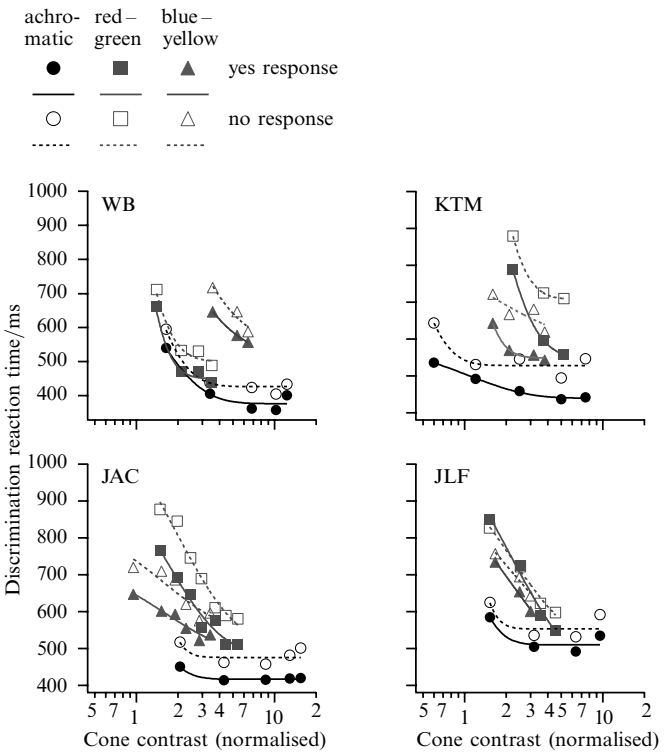

(a) Straight-path discrimination

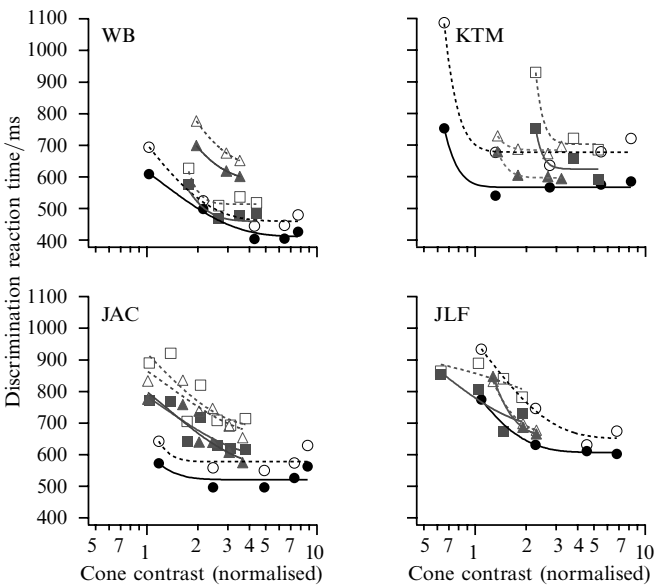

(b) Curved-path discrimination

Figure 4. Discrimination reaction times as a function of contrast for all four subjects. Reaction times for path discrimination for straight (a) and curved (b) conditions expressed as a function of multiple of cone contrast thresholds for path detection (normalised cone contrast). Circles, squares, and triangles represent reaction times for achromatic, red – green, and blue – yellow stimuli, respectively. Plain and open symbols represent measurements of reaction times for detection of path presence and path absence, respectively. Solid and dashed lines denote fits for path presence and path absence data, respectively.

In some conditions, reaction times for red–green and blue–yellow stimuli show no asymptotic behaviour at all.

Rather than fitting asymptotic reaction times with equation (2), reaction times at the same multiple of path-detection threshold ($\times 3.5$ for all subjects, except for JLF whose highest multiple is $\times 2$) were averaged across subjects and are shown in figure 5. As before, we applied a one-way repeated-measures ANOVA to analyse the differences in reaction time across conditions (curved and straight paths, present and absent) for each postreceptoral mechanism. In each case we find a significant main effect of condition ($F_{3,9} = 15.047$, $p = 0.0007$ for achromatic stimuli; $F_{3,9} = 6.811$, $p = 0.0108$ for red–green stimuli; $F_{3,9} = 4.620$, $p = 0.0321$ for blue–yellow stimuli). Differences among conditions were further explored with a Tukey–Kramer a posteriori analysis with a 5% significance level which showed that: (1) for the luminance mechanism, discrimination reaction time is significantly longer for the curved paths compared with the straight paths (by about 100–125 ms) irrespective of whether the path is present or absent, and (2) for all three postreceptoral mechanisms, the detection of path absence is significantly slower than detection of path presence (by 50–80 ms) irrespective of path curvature. We also collapsed data across conditions (curved and straight paths, present and absent) and applied a further one-way repeated-measures ANOVA to test differences in discrimination reaction times between the three mechanisms. A significant main effect of chromatic mechanism was found ($F_{2,30} = 14.761$, $p < 0.0001$). Differences between mechanisms were further explored with a Tukey–Kramer a posteriori analysis with a 5% significance level which showed that discrimination reaction times for achromatic stimuli are significantly shorter than for either red–green (by 91 ms) or blue–yellow (by 105 ms) stimuli, with no significant differences between discrimination reaction times for blue–yellow and red–green stimuli.

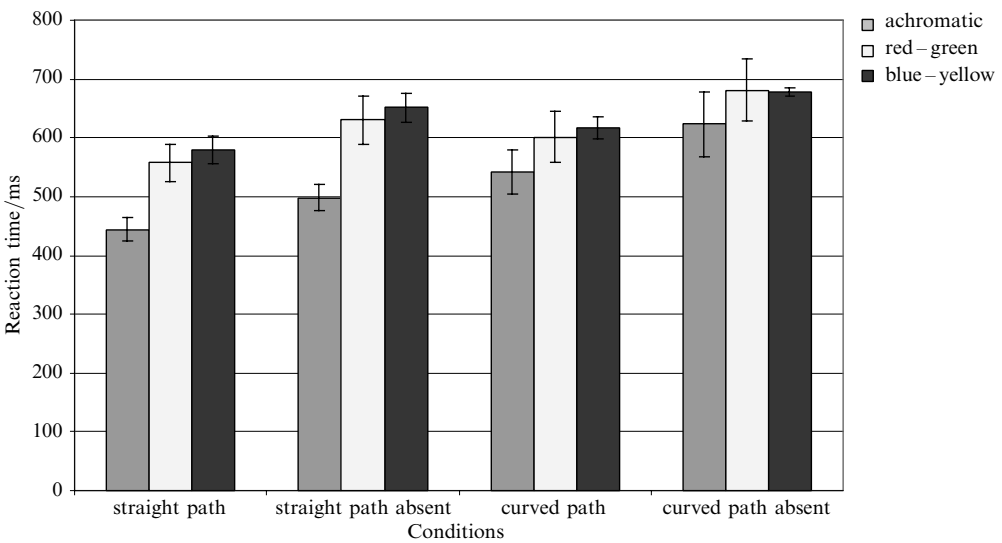

Figure 5. Averaged discrimination reaction times across subjects at a multiple of path-detection threshold. Each experimental condition is represented from left to right: presence of straight path, absence of straight path, presence of curved path, absence of curved path. Error bars denote standard errors of the means.

3.3 *Additional processing time for path detection*

Additional processing times for contour integration as a function of contrast are calculated as the difference between data points for discrimination reaction times (figure 4) and simple reaction times (figure 2), and are shown in figure 6 by data points

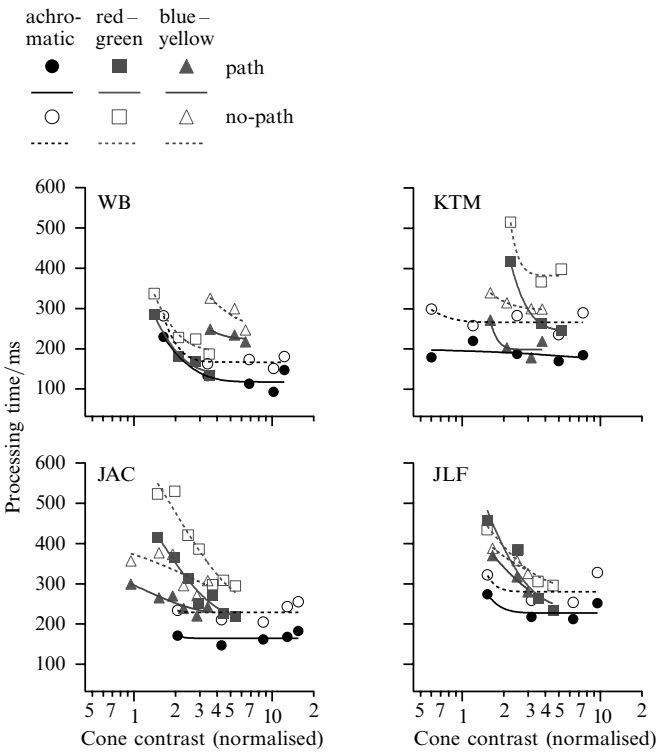

(a) Straight-path processing

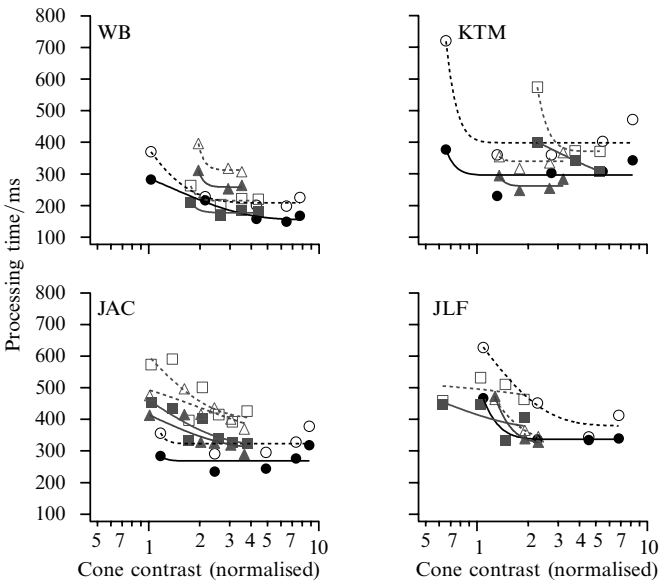

(b) Curved-path processing

Figure 6. Additional processing times as a function of contrast for all four subjects. Additional processing times for path discrimination for straight (a) and curved (b) conditions are expressed as a function of multiple cone contrast thresholds for path detection (normalised cone contrast). Additional processing times were computed as the difference between reaction times for path discrimination (figure 4) and simple stimulus detection (figure 2). Circles, squares, and triangles represent processing times for achromatic, red – green, and blue – yellow stimuli, respectively. Plain and open symbols represent processing times for detection of path presence and path absence, respectively. Solid and dashed lines denote fits for path presence and path absence data, respectively.

with solid and dashed curves denoting fits by equation (2). Processing times are expressed as a function of multiples of cone contrast thresholds. Similar to path-discrimination reaction times, processing times for the chromatic mechanisms show an initial steep decrease with increasing contrast, followed, however, by a much clearer asymptotic level at suprathreshold contrasts. As for the achromatic mechanism, processing times are rather flat or show a more or less accentuated U-shape. Processing times for achromatic stimuli are generally slightly shorter than processing times for chromatic stimuli, with no consistent difference between red – green and blue – yellow stimuli.

Fitted asymptotic processing times were averaged across subjects (data not shown). We also considered processing times at multiples of path-detection threshold ($\times 3.5$ for all subjects, except $\times 2$ for JLF) averaged across subjects (figure 7), as well as minimum processing times for the achromatic data fitted by a difference of exponentials (data not shown). We applied the following statistical analysis to all sets of data (results for multiples of path-detection threshold and minimum processing times are not presented in the text, but are included in table 1 for comparison with results for asymptotic processing times). As before, we applied a one-way repeated-measures ANOVA to analyse the differences in processing time across conditions (curved and straight paths, present and absent) for each postreceptoral mechanism. In each case we find a significant main effect of condition ($F_{3,9} = 25.325$, $p = 0.0001$ for achromatic stimuli; $F_{3,9} = 6.507$, $p = 0.0124$ for red – green stimuli; $F_{3,9} = 14.846$, $p = 0.0008$ for blue – yellow stimuli). Differences among conditions were further explored with a Tukey – Kramer a posteriori analysis with a 5% significance level which showed that for all three postreceptoral mechanisms: (i) processing time for curved-path detection is significantly longer than for straight-path detection by 93, 73, and 60 ms for achromatic, red – green, and blue – yellow stimuli, respectively, irrespective of whether the path is present or absent, and (ii) processing time for detection of path absence is significantly longer than for detection of path presence by 50 – 68 ms, irrespective of path curvature.

We also collapsed data across conditions for each curvature and applied a further one-way repeated-measures ANOVA to test differences in processing times between the three chromatic mechanisms. A significant main effect of chromatic mechanism was

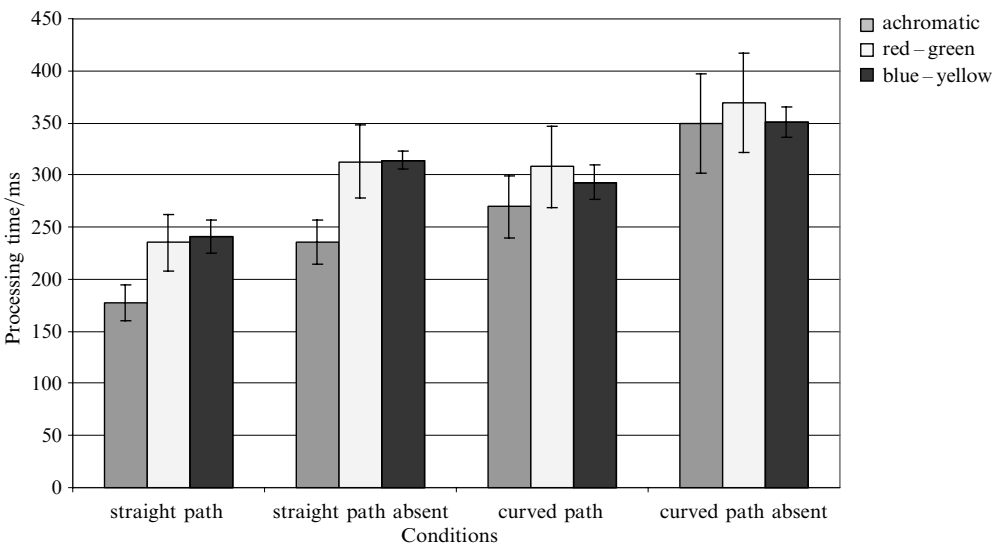

Figure 7. Averaged additional processing times for path detection across subjects at a multiple of the path-detection threshold. Each experimental condition is represented from left to right: presence of straight path, absence of straight path, presence of curved path, absence of curved path. Error bars denote standard errors of the means.

found for straight paths only ($F_{2,14} = 5.292$, $p = 0.0194$) and was further explored with a Tukey–Kramer a posteriori analysis (5% significance level). This showed that (for straight paths) processing time for achromatic paths is significantly shorter than for chromatic ones by at least 40 ms, with no significant differences between blue–yellow and red–green stimuli. For curved paths, there are no differences in processing times between the three mechanisms, suggesting a longer iterative process applied equally across mechanisms. Note that the different possible ways we could define the contrast-independent processing time (asymptotic, minimum, or at multiple of threshold) do not affect our conclusions, as shown by table 1.

Table 1. Table showing the statistics on additional processing times (PTs) compared according to three definitions (asymptotic PT—by fitting a decreasing exponential, PT at multiples of threshold, and minimum PT—by fitting a difference of exponentials). Differences in processing times between curvature conditions are presented in the row entitled PT difference ($20^\circ - 0^\circ$ conditions). Ranges (across mechanisms) of the difference in processing times between absence and presence conditions are presented in the row entitled PT difference (absence–presence conditions). Statistics showing the significant effect of the achromatic mechanism on the straight-path condition are shown in the bottom part of the table.

ANOVAs results	Asymptotic PT	PT at multiple thresholds	Minimum PT
Achromatic stimuli			
$F_{3,9}$	25.325	20.365	31.853
p	0.0001	0.0002	< 0.0001
PT difference ($20^\circ - 0^\circ$ conditions)	93 ms	103 ms	81 ms
Red–green stimuli			
$F_{3,9}$	6.507	10.656	–
p	0.0124	0.0026	–
PT difference ($20^\circ - 0^\circ$ conditions)	73 ms	65 ms	–
Blue–yellow stimuli			
$F_{3,9}$	14.846	12.699	–
p	0.0008	0.0014	–
PT difference ($20^\circ - 0^\circ$ conditions)	60 ms	44 ms	–
PT difference (absence–presence conditions)	50–68 ms	58–80 ms	52–68 ms
Effect of mechanisms on straight-path condition			
$F_{2,14}$	5.292	7.672	10.572
p	0.0194	0.0056	0.0016
Achromatic PT advantage	40 ms	70 ms	60 ms

3.4 *Extra processing time for curvature difference and no-path detection*

In this section we further quantify the increases in additional processing times found for the curved as opposed to straight paths, and for detecting the absence of a path compared to its presence, for the achromatic, red–green, and blue–yellow stimuli. 'Extra processing time' is calculated as the difference between processing times for curved and straight path detection and between processing times for detection of path absence and path presence.

On the basis of the data in figure 6, we initially calculated extra processing times for each postreceptoral mechanism and condition as a function of contrast. These results, however, showed no consistent trend as a function of contrast and so in the subsequent analyses we collapsed the extra processing times across contrast for each

subject and condition. We first applied two separate one-way repeated-measures ANOVAs to these data for each chromatic mechanism for each subject to show that there is: (i) no significant effect of path presence/absence on the extra processing times required for curved paths, and (ii) no significant effect of curvature on the extra processing times required for the detection of path absence. We then combined data across path conditions and subjects (figure 8a), and across curvature and subjects (figure 8b), and applied two further separate one-way repeated-measures ANOVAs to test differences in extra processing times between the three chromatic mechanisms. A significant main effect of chromatic mechanism was found for the extra processing times for curvature ($F_{2,54} = 10.963$, $p = 0.0001$) (figure 8a), but none for extra processing time for path absence ($F_{2,54} = 0.701$, $p = 0.5007$) (figure 8b). Differences between mechanisms were further explored with a Tukey–Kramer a posteriori analysis at the 5% significance level which showed that the extra processing time required for curved paths is significantly greater for achromatic stimuli than for either red–green (by about 82 ms) or blue–yellow stimuli (by about 60 ms). There is no significant difference in extra processing time between blue–yellow and red–green stimuli.

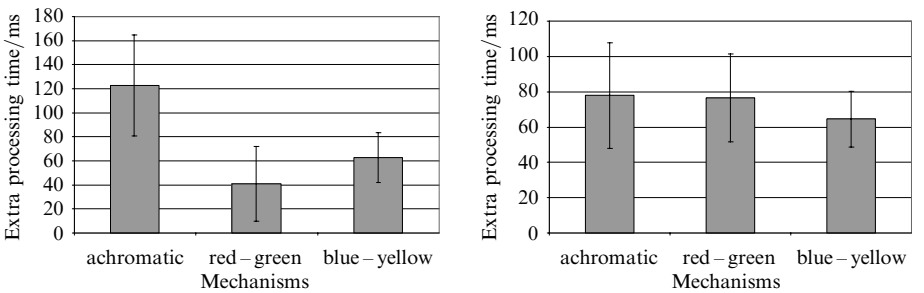

(a) Extra processing times for curved-path detection (b) Extra processing times for detection of path absence

Figure 8. Averaged extra processing times across contrasts and subjects. Extra processing times for (a) the curvature increase and (b) detection of path absence (relatively to detection of path presence) for each postreceptoral mechanism were derived from data of figure 6. Error bars denote standard errors of the means.

3.5 *Summary of the findings*

On the basis of the averaged asymptotic reaction-time measurements or the averaged reaction times at a multiple of path-detection threshold we find:

(1) Reaction times for simple stimulus detection are shortest for achromatic stimuli, about 30 ms longer for red–green stimuli, and about 30 ms longer again for blue–yellow stimuli.

(2) Reaction times for path detection are shorter (up to 100 ms) for achromatic stimuli than for chromatic stimuli, with no significant differences between blue–yellow and red–green stimuli. However, reaction times for achromatic stimuli are longer (by around 100–125 ms) for curved-path detection than for straight-path detection. Detection of path absence is slower (by 50–80 ms) than detection of path presence.

(3) Additional processing times for contour integration, calculated as the difference between (1) and (2) above, are longer (by 50–100 ms) for curved paths than for straight paths, and are longer for the detection of path absence (by 50–70 ms) than path presence. For straight paths, the achromatic mechanism is faster than the chromatic ones (by 40–70 ms), with no difference between red–green and blue–yellow mechanisms. For curved paths there is no difference in processing time between mechanisms.

(4) The extra processing time required to detect curved compared with straight paths is longest for the achromatic mechanism (by 60–82 ms), and similar for the red–green and blue–yellow mechanisms.

4 Discussion

4.1 *Differing perceptual latencies*

The lack of dependence of simple reaction times on curvature suggests, as expected, that simple detection does not involve processing related to stimulus content (ie orientation or form). We found, however, absolute differences in average simple reaction time between the postreceptoral mechanisms, with the luminance mechanism being the fastest and the blue–yellow mechanism being the slowest. These reaction times also showed a specific distribution, with the luminance system peaking sooner and with a narrower distribution than those for the chromatic systems (data not shown). These findings are consistent with previous reports on temporal properties of the two systems and the psychophysical findings that the chromatic system is temporally lowpass and more sluggish than the achromatic system (Bowen 1981; Kelly 1983; Metha and Mullen 1996; Schwartz and Loop 1982). The reaction times we measured for achromatic stimuli as a function of contrast asymptote between 250 and 300 ms, and are in accordance with previous studies which made use of gratings (Ejima and Ohtani 1987; Felipe et al 1993; Thomas et al 1999). Recent results from visual evoked potential (VEP) and magnetoencephalogram (MEG) studies also support the longer visual latencies we found for chromatic red–green compared with achromatic stimuli (by about 20–40 ms) (Fiorentini et al 1991; Girard and Morrone 1995; Klistorner et al 1998; Regan and He 1996), this difference being partially explained at a retinal level (Morrone et al 1994a, 1994b; Porciatti et al 1994). Curiously, the significant difference in simple reaction times we found between red–green and blue–yellow mechanisms was not found in a previous study measuring MEG responses, which reported no differences between the two chromatic systems (Regan and He 1996). There remains disagreement about whether VEP responses of the blue–yellow and red–green systems are similar (Kulikowski et al 1989) or different (Berninger et al 1989). Our result is, however, in accordance with single-cell recordings of latencies in V1 of the macaque which show that S-cone opponent neurons have a greater latency than L/M cone opponent ones (20–30 ms), a difference thought to originate in the cortex itself (Cottaris and De Valois 1998).

4.2 *Significance of differing processing times*

Unlike simple reaction times, path-discrimination reaction times show significant differences as a function of curvature, reflecting the additional time demands of contour integration after the initial perceptual latency. We estimated the additional processing times for contour integration by subtracting simple reaction times from discrimination reaction times. This subtraction eliminates the initial perceptual latency, including the effects of the transmission time, detection integration time, and the delay in motor response, but not any difference in decision time between simple and path detections. In the case of simple stimulus detection, however, decision time, if significant, is expected to be constant across conditions once the stimulus reaches the detection threshold. In the case of path discrimination, decision time for interpreting the stimulus depends on the presence of a path, the detection of path absence requiring a decision process ascertaining the lack of response from the contour-integration stage. We found, indeed, that the detection of path absence requires about 50–80 ms of additional time independent of chromaticity, contrast, or path curvature. In other words, if the subjects know they are looking for a curved path they take longer overall to decide it is absent than if they know they are looking for a straight path. The extra processing time required for curved paths appears to arise from the curvature detectors involved in the visual-search task, regardless of whether they are actually successful at identifying a path.

Although we are assuming that all curvature conditions are processed in the same way, it remains a possibility that observers may not base their decision on the same number of elements in the straight-path and curved-path conditions. For example, straight-path detection might be made when integration has only partially been completed, or a curved path may require the detection of more elements than a straight path, which may explain why straight paths are detected faster than curved paths. However, this is unlikely for the following reasons: (i) we know that contour integration cannot be performed on the basis of only five alternative elements whatever the curvature (McIlhagga and Mullen 1996); (ii) the use of fewer path elements decreases performance; and (iii) a straight path is always perceived very distinctly with all its elements.

It is still possible that other higher-level or cognitive processes influence the estimated additional processing time but they are expected to be minimised since the subjects were experienced with the task, were asked to respond as fast as possible, and knew the curvature of the paths they had to detect. Our assumptions rely on several parsimonious hypotheses: (i) all path elements are processed in parallel and are used for its detection; (ii) simple detection is accomplished by early cortical processing, presumably thresholding of V1 neuronal activity; (iii) these neurons provide the subsequent signal to higher cortical stages handling orientation linking; (iv) the decision processes which trigger the motor response perform the same function in simple detection and path detection, ie they should take the same amount of time and be independent of chromaticity and curvature. Thus we are reasonably confident that the calculation of additional processing time reflects the time required for the contour-integration process, including decision time specific to path detection.

4.3 *The dynamics of curvature processing*

Field et al (1993) proposed an association field, which describes the spatial rules governing the linking of path elements into a contour. They postulated that path detection depends on local interactions and integrative processes among cortical neurons that analyse different orientations in different regions of visual space, and not on a simple filtering model (Hess and Dakin 1997). This two-stage process, local edge detection followed by boundary integration of adjacent elements with similar orientation changes, is used in a number of computational approaches to image segmentation (Grossberg and Mingolla 1985; Heitger and von der Heydt 1993). However, from a computational point of view, this process, performed in parallel across space, cannot be instantaneous since it has an optimisation problem to solve owing to the stochastic nature of the stimulus. None of the current models of contour integration (Grossberg 1999; Heitger et al 1992; Li 1998, 1999; Williams and Jacobs 1997; Yen and Finkel 1998) has incorporated explicitly any dynamics.

We find that additional processing time for contour integration is modulated by curvature, being considerably longer for curved compared with straight paths. This result is consistent with a recent study which used a masking paradigm to assess the dynamics of contour integration for achromatic stimuli (Hess et al 2001). Thus our finding unveils one important aspect of the dynamics of the association field: contour integration may arise from a dynamic process initially tuned to straight paths and temporally evolving to match the spatial properties of the path. This process could have implicit dynamics or could be simply driven by feedforward inputs from multiple static detectors tuned to different curvatures, the ones tuned to straighter paths being faster than the ones tuned to curved paths. It is often assumed that response latencies reflect different visual processing levels, with the longer reaction times for curved paths indicating the involvement of higher levels in the cortical hierarchy of the visual system (Barbur et al 1998). However, we favour a single mechanism with intrinsic curvature-dependent dynamics. The 50 – 100 ms difference between the straight-path and the

curved-path conditions is long enough to allow both intracortical and extracortical interactions in the visual cortex to take part in an optimisation process, which is compatible with recent evidence for the role of intracortical and extracortical feedback in figure–ground segregation (Budd 1998; Lamme et al 1998), and the modulatory effects of global context on local processing (Gilbert 1997; Zipser et al 1996).

The curvature-dependent dynamics revealed by our results are reminiscent of previous models proposed for visual segmentation (Li 1999; Mesrobian and Skrzypek 1995; Wang and Terman 1997), and could be explained by one of the models described by Yen and Finkel (1998), which involves a context-dependent change in long-range connections so as to optimally tune each cell's input to the structure of the surround. They suggest that the connectivity pattern may be dynamically potentiated by the surrounding elements so as to steer the connections to suit the context. However, the authors did not suggest how this mechanism could coherently operate to achieve the context-dependent changes they described. The missing links are to access the context and to modulate the connectivity pattern defined by the long-range connections, which would require a higher-order integrative process acting in feedback on the local interactions between cortical neurons analysing different orientations. The orientation properties modulated by this hypothetical linking process require some orientation dynamics that parallel the curvature-dependent dynamics of contour integration. This scheme may carry out the boundary-integration stage of the two-stage process of the computational approaches.

There is good physiological and psychophysical evidence to support the existence of cortical dynamics for orientation processing. Several studies have demonstrated that orientation tuning of cortical neurons develops or changes continuously over time (Ringach et al 1997; Shevelev et al 1993; Volgushev et al 1995) (but see Celebrini et al 1993), and psychophysical results show that, at low spatial frequencies, increasing temporal frequency progressively increases orientation bandwidth (Snowden 1992). In an investigation of the visual mechanisms underlying rapid orientated-line detection, Foster and Westland (1998) found a temporal shift in balance of activity between groups of orientation-selective mechanisms from coarse to intermediate and fine, suggesting that the visual system performs a 'coarse-to-fine' analysis of orientation information. Exactly how these mechanisms might be involved in contour integration is unclear. Nevertheless, cortical neurons with dynamic orientation tuning modulated by contextual surround could clearly play a role in the dynamic association field mechanism we described for contour integration.

Our results also show that the effect of curvature is differential for achromatic and chromatic stimuli. Additional processing times are significantly shorter for achromatic stimuli compared with chromatic stimuli in the straight-path condition, but are similar in the curved-path condition. As a consequence, the effect of curvature appears to be greatest for achromatic stimuli, increasing processing time by more than 100 ms compared to only 40–60 ms for chromatic stimuli. The shorter processing time for achromatic straight-path detection may indicate a more reliable neural encoding of luminance contrast, while the differential curvature-dependent dynamics might reflect differences in processing of orientation between the colour and luminance systems. Psychophysical data suggest that orientation processing, at least at threshold, is poorer in the chromatic systems (Bradley et al 1988; Mullen et al 2000; Pandey Vimal 1997; Webster et al 1990). To cover the orientation domain may require more narrow orientation-tuned achromatic detectors, and fewer broad orientation-tuned chromatic detectors. The difference in number of orientation samples for achromatic and chromatic detectors might result in a more ambiguous processing for luminance than for chromatic mechanisms for contour integration. A temporal iterative processing solving the ambiguity of linking orientation across space may then need more

time to converge for the luminance mechanism than for the chromatic mechanisms with an increase in curvature.

4.4 *Chromatic selective linking as a consequence of different temporal properties?*
In a previous study, we have shown that contour integration by each postreceptoral mechanism has very similar spatial properties, suggesting that the three mechanisms share a common contour-integration process (Mullen et al 2000). This common process, however, must remain sensitive to the chromaticity of its inputs because the detection of paths that alternate the colour of their elements is severely impaired (McIlhagga and Mullen 1996; Mullen et al 2000). However, neither an independent-channels model, nor a cross-sensitivity model offers an explanation for this reduction in contour detectability (McIlhagga and Mullen 1996). One possibility is that the different temporal properties of the three postreceptoral mechanisms may affect the ability to link orientation between mechanisms. In particular, simultaneous neural activations might be more effective as inputs for the linking process than asynchronous activations which might be responsible for the disruptive effect on contour integration of linking between different chromatic elements. We reported in this paper two potential sources for such asynchrony between luminance and chromatic mechanisms which could contribute to feature binding in visual segmentation (Gawne et al 1996): their differing perceptual latencies and differing curvature-dependent processing times. However, although attractive, the hypothesis that the linking process may retain the colour selectivity of its inputs, or at least their timing differences, remains to be directly tested.

Acknowledgements. This study was funded by a grant from the Medical Research Council of Canada to K T Mullen (MT-10819) and by a fellowship from the Fyssen Foundation to W H A Beaudot. We acknowledge partial support from the Réseau FRSQ de Recherche en Santé de la Vision. The authors also thank Jennifer Chow for help in collecting data.

References

Anstis S, Cavanagh P, 1983 "A minimum motion technique for judging equiluminance", in *Color Vision: Physiology and Psychophysics* Eds J D Mollon, L T Sharpe (London: Academic Press) pp 155 – 166

Barbur J L, Wolf J, Lennie P, 1998 "Visual processing levels revealed by response latencies to changes in different visual attributes" *Proceedings of the Royal Society of London, Series B* **265** 2321 – 2325

Beaudot W H A (submitted) "Role of onset asynchrony in contour integration" *Vision Research*

Berninger T A, Arden G B, Hogg C R, Frumkes T, 1989 "Separable evoked retinal and cortical potentials from each major visual pathway: preliminary results" *British Journal of Ophthalmology* **73** 502 – 511

Bowen R W, 1981 "Latencies for chromatic and achromatic visual mechanisms" *Vision Research* **21** 1457 – 1466

Bradley A, Switkes E, De Valois K K, 1988 "Orientation and spatial frequency selectivity of adaptation to color and luminance gratings" *Vision Research* **28** 841 – 856

Braun J, 1999 "On the detection of salient contours" *Spatial Vision* **12** 211 – 225

Braun J, Niebur E, Schuster H G, Koch C, 1994 "Perceptual contour completion: a model based on local anisotropic, fast-adapting interactions between oriented filters", in *Society for Neuroscience Abstracts* **20**(1 – 2) 1665

Budd J M, 1998 "Extrastriate feedback to primary visual cortex in primates: a quantitative analysis of connectivity" *Proceedings of the Royal Society of London, Series B* **265** 1037 – 1044

Burr D C, Fiorentini A, Morrone C, 1998 "Reaction time to motion onset of luminance and chromatic gratings is determined by perceived speed" *Vision Research* **38** 3681 – 3690

Celebrini S, Thorpe S, Trotter Y, Imbert M, 1993 "Dynamics of orientation coding in area V1 of the awake primate" *Visual Neuroscience* **10** 811 – 825

Cole G R, Hine T, 1992 "Computation of cone contrasts for color vision research" *Behavioural Research, Methods and Instrumentation* **24** 22 – 27

Cole G R, Hine T, McIlhagga W, 1993 "Detection mechanisms in L-, M-, and S-cone contrast space" *Journal of the Optical Society of America A* **10** 38 – 51

Cottaris N P, De Valois R L, 1998 "Temporal dynamics of chromatic tuning in macaque primary visual cortex" *Nature* **395** 896 – 900

Dakin S C, Hess R F, 1998 "Spatial-frequency tuning of visual contour integration" *Journal of the Optical Society of America A* **15** 1486 – 1499

Dakin S C, Hess R F, 1999 "Contour integration and scale combination processes in visual edge detection" *Spatial Vision* **12** 309 – 327

Donders F C, 1868 "On the speed of mental processes", translated by W G Koster, 1969 *Acta Psychologica* **30** 412 – 431

Ejima Y, Ohtani Y, 1987 "Simple reaction time to sinusoidal grating and perceptual integration time: contributions of perceptual and response processes" *Vision Research* **27** 269 – 276

Elder J, Zucker S, 1993 "The effect of contour closure on the rapid discrimination of two- dimensional shapes" *Vision Research* **33** 981 – 991

Felipe A, Buades M J, Artigas J M, 1993 "Influence of the contrast sensitivity function on the reaction time" *Vision Research* **33** 2461 – 2466

Field D J, Hayes A, Hess R F, 1993 "Contour integration by the human visual system: evidence for a local 'association field' " *Vision Research* **33** 173 – 193

Fiorentini A, Burr D C, Morrone C, 1991 "Spatial and temporal characteristics of colour vision: VEP and psychophysical measurements", in *From Pigments to Perception: Advances in Understanding Visual Processing* Eds A Valberg, B B Lee (New York: Plenum Press) pp 139 – 150

Foster D H, Westland S, 1998 "Multiple groups of orientation-selective visual mechanisms underlying rapid orientated-line detection" *Proceedings of the Royal Society of London, Series B* **265** 1605 – 1613

Gawne T J, Kjaer T W, Richmond B J, 1996 "Latency: another potential code for feature binding in striate cortex" *Journal of Neurophysiology* **76** 1356 – 1360

Gilbert C D, 1997 "Cortical dynamics" *Acta Paediatrica* **422** Supplement, 34 – 37

Girard P, Morrone M C, 1995 "Spatial structure of chromatically opponent receptive fields in the human visual system" *Visual Neuroscience* **12** 103 – 116

Greenlee M W, Breitmeyer B G, 1989 "A choice reaction time analysis of spatial frequency discrimination" *Vision Research* **29** 1575 – 1586

Grossberg S, 1999 "How does the cerebral cortex work? Learning, attention, and grouping by the laminar circuits of visual cortex" *Spatial Vision* **12** 163 – 185

Grossberg S, Mingolla E, 1985 "Neural dynamics of perceptual grouping: textures, boundaries, and emergent segmentations" *Perception & Psychophysics* **38** 141 – 171

Heitger F, Heydt R von der, 1993 "A computational model of neural contour processing: Figure – ground segregation and illusory contours", in *Proceedings of the 4th International Conference on Computer Vision, Berlin* (Los Alamitos, CA: IEEE Computer Society Press) pp 32 – 40

Heitger F, Rosenthaler L, Heydt R von der, Peterhans E, Kubler O, 1992 "Simulation of neural contour mechanisms: from simple to end-stopped cells" *Vision Research* **32** 963 – 981

Hess R F, Dakin S C, 1997 "Absence of contour linking in peripheral vision" *Nature* **390** 602 – 604

Hess R F, Beaudot W H A, Mullen K T, 2001 "Dynamics of contour integration" *Vision Research* in press

Kapadia M K, Ito M, Gilbert C D, Westheimer G, 1995 "Improvement in visual sensitivity by changes in local context: parallel studies in human observers and in V1 of alert monkeys" *Neuron* **15** 843 – 856

Kelly D H, 1983 "Spatiotemporal variation of chromatic and achromatic contrast thresholds" *Journal of the Optical Society of America A* **73** 742 – 750

Klistorner A, Crewther D P, Crewther S G, 1998 "Temporal analysis of the chromatic flash VEP—separate colour and luminance contrast components" *Vision Research* **38** 3979 – 4000

Kovacs I, Julesz B, 1993 "A closed curve is much more than an incomplete one: effect of closure in figure – ground segmentation" *Proceedings of the National Academy of Sciences of the USA* **90** 7495 – 7497

Kulikowski J J, Murray I J, Parry N R A, 1989 "Electrophysical correlates of chromatic-opponent and achromatic stimulation in man", in volume IX of *Colour Vision Deficiencies* Eds B Drum, G Verriest (Dordrecht: Kluwer) pp 145 – 153

Külpe O, 1893 *Grundriss der Psychologie. Auf experimenteller Grundlage dargestellt* (Leipzig: Wilhelm Engelmann), translated by E B Titchener as Külpe O, 1895 *Outlines of Psychology Based upon the Results of Experimental Investigation* (London: Swan Sonnenschein)

Lamme V A, Super H, Spekreijse H, 1998 "Feedforward, horizontal, and feedback processing in the visual cortex" *Current Opinion in Neurobiolology* **8** 529 – 535

Li Z, 1998 "A neural model of contour integration in the primary visual cortex" *Neural Computation* **10** 903 – 940

Li Z, 1999 "Visual segmentation by contextual influences via intra-cortical interactions in the primary visual cortex" *Network-Computation in Neural Systems* **10** 187 – 212
McIlhagga W H, Mullen K T, 1996 "Contour integration with colour and luminance contrast" *Vision Research* **36** 1265 – 1279
Mesrobian E, Skrzypek J, 1995 "Segmenting textures using cells with adaptive receptive fields" *Spatial Vision* **9** 163 – 190
Metha A B, Mullen K T, 1996 "Temporal mechanisms underlying flicker detection and identification for red – green and achromatic stimuli" *Journal of the Optical Society of America A* **13** 1969 – 1980
Morrone C, Porciatti V, Fiorentini A, Burr D C, 1994a "Pattern-reversal electroretinogram in response to chromatic stimuli: I. Humans" *Visual Neuroscience* **11** 861 – 871
Morrone C, Fiorentini A, Bisti S, Porciatti V, Burr D C, 1994b "Pattern-reversal electroretinogram in response to chromatic stimuli: II. Monkey" *Visual Neuroscience* **11** 873 – 884
Mullen K T M, Beaudot W H A, McIlhagga W H, 2000 "Contour integration in color vision: a common process for the blue – yellow, red – green and luminance mechanisms?" *Vision Research* **40** 639 – 655
Pandey Vimal R L, 1997 "Orientation tuning of the spatial-frequency-tuned mechanisms of the red – green channel" *Journal of the Optical Society of America A* **14** 2622 – 2632
Parent P, Zucker S, 1989 "Trace inference, curvature consistency and curve detection" *IEEE Transactions on Pattern Analysis and Machine Intelligence* **PAMI-6** 661 – 675
Pettet M W, 1999 "Shape and contour detection" *Vision Research* **39** 551 – 557
Pettet M W, McKee S P, Grzywacz N M, 1998 "Constraints on long range interactions mediating contour detection" *Vision Research* **38** 865 – 879
Porciatti V, Morrone M C, Fiorentini A, Burr D C, Bisti S, 1994 "The pattern electroretinogram in response to colour contrast in man and monkey" *International Journal of Psychophysiology* **16** 185 – 189
Regan D, He P, 1996 "Magnetic and electrical brain responses to chromatic contrast in human" *Vision Research* **36** 1 – 18
Ringach D L, Hawken M J, Shapley R, 1997 "Dynamics of orientation tuning in macaque primary visual cortex" *Nature* **387** 281 – 284
Roelfsema P R, Singer W, 1998 "Detecting connectedness" *Cerebral Cortex* **8** 385 – 396
Sankeralli M J, Mullen K T, 1996 "Estimation of the L-, M-, and S-cone weights of the post-receptoral detection mechanisms" *Journal of the Optical Society of America A* **13** 906 – 915
Schwartz S H, Loop M S, 1982 "Evidence for luminance and quasi-sustained color mechanisms" *Vision Research* **22** 445 – 447
Shashua A, Ullman S, 1988 "Structural saliency: the detection of globally salient structures using a locally connected network", in *Proceedings of the 2nd International Conference on Computer Vision, Tarpon Springs, FL* (Los Alamitos, CA: IEEE Computer Society Press) pp 321 – 327
Shevelev I A, Sharaev G A, Lazareva N A, Novikova R V, Tikhomirov A S, 1993 "Dynamics of orientation tuning in the cat striate cortex neurons" *Neuroscience* **56** 865 – 876
Smith V C, Pokorny J, 1975 "Spectral sensitivity of the foveal cone photopigments between 400 and 500 nm" *Vision Research* **15** 161 – 171
Snowden R J, 1992 "Orientation bandwidth: the effect of spatial and temporal frequency" *Vision Research* **32** 1965 – 1974
Thomas J P, Fagerholm P, Bonnet C, 1999 "One spatial filter limits speed of detecting low and middle frequency gratings" *Vision Research* **39** 1683 – 1693
Volgushev M, Vidyasagar T R, Pei X, 1995 "Dynamics of the orientation tuning of postsynaptic potentials in the cat visual cortex" *Visual Neuroscience* **12** 621 – 628
Wang D, Terman D, 1997 "Image segmentation based on oscillatory correlation" *Neural Computation* **9** 805 – 836
Webster M A, De Valois K K, Switkes E, 1990 "Orientation and spatial-frequency discrimination for luminance and chromatic gratings" *Journal of the Optical Society of America A* **7** 1034 – 1049
Williams C B, Hess R F, 1998 "Relationship between facilitation at threshold and suprathreshold contour integration" *Journal of the Optical Society of America A* **15** 2046 – 2051
Williams L R, Jacobs D W, 1997 "Stochastic completion fields; a neural model of illusory contour shape and salience" *Neural Computation* **9** 837 – 858
Yen S C, Finkel L H, 1998 "Extraction of perceptually salient contours by striate cortical networks" *Vision Research* **38** 719 – 741
Zipser K, Lamme V A, Schiller P H, 1996 "Contextual modulation in primary visual cortex" *Journal of Neuroscience* **16** 7376 – 7389